Bull. Mater. Sci., Vol. 36, No. 7, December 2013, pp. 1281–1290. © Indian Academy of Sciences.

Electrochemical copolymerization of *N*-methylpyrrole and 2,2′-bithitiophene; characterization, micro-capacitor study, and equivalent circuit model evaluation

MURAT ATES[1,*], FATIH ARICAN[1] and TOLGA KARAZEHIR[1,2]

[1]Department of Chemistry, Faculty of Arts and Sciences, Namik Kemal University, Degirmenalti Campus, Tekirdag 59030, Turkey

[2]Department of Chemistry, Faculty of Arts and Sciences, Istanbul Technical University, Maslak, Istanbul, Turkey

MS received 29 July 2012; revised 4 November 2012

Abstract. ***N*-methylpyrrole (*N*-MPy) and 2,2′-bithiophene (BTh) were electrocopolymerized in 0·2 M acetonitrile–sodium perchlorate solvent–electrolyte couple on a glassy carbon electrode (GCE) by cyclic voltammetry (CV). The resulting homopolymers and copolymers in different initial feed ratios of $[N\text{-MPy}]_0/[\text{BTh}]_0 = 1/1, 1/2, 1/5$ and 1/10 were characterized by CV, Fourier-transform infrared reflectance attenuated transmittance (FTIR–ATR), scanning electron microscopy (SEM), energy dispersive X-ray analysis (EDX) and electrochemical impedance spectroscopy (EIS). The capacitive behaviours of the modified electrodes were defined via Nyquist, Bode-magnitude, Bode-phase and admittance plots. The equivalent circuit model of R(C(R)(QR)(CR)) was performed to fit theoretical and experimental data. The highest low-frequency capacitance (C_{LF}) were obtained as $C_{LF} = \sim 1{\cdot}23 \times 10^{-4}$ mF cm^{-2} for P(N-MPy), $C_{LF} = \sim 2{\cdot}09 \times 10^{-4}$ mF cm^{-2} for P(BTh) and $C_{LF} = \sim 5{\cdot}54 \times 10^{-4}$ mF cm^{-2} for copolymer in the inital feed ratio of $[N\text{-MPy}]_0/[\text{BTh}]_0 = 1/2$.**

Keywords. ***N*-methylpyrrole; 2,2′-bithitiophene; copolymers; electrochemical impedance spectroscopy; conducting polymers; circuit model.**

1. Introduction

For the last thirty years, conducting polymers have attracted considerable interest for the development of advanced materials due to the structure and property of the polymer, which changes from a doped state as a conductor or an undoped (neutral) state as an insulator or semiconductor (McCullough 1998; Skotheim *et al* 1998; Zhang *et al* 1999, 2000). These compounds are organic materials that generally possess an extended conjugated π-electron system along a polymer backbone, such as polypyrroles (PPy) (De Bruyne *et al* 1997; Volpi *et al* 2012), polyanilines (Dalmolin *et al* 2005; Tuan *et al* 2012), polycarbazoles (Saraswathi *et al* 1999; Zhoor *et al* 2009; Pokhnel *et al* 2012) and polythiophenes (Akoudad and Roncali 1999; Mahmoudian *et al* 2011; Alvi *et al* 2012).

Polypyrrole (PPy) (Mollahosseini and Noroozian 2009; Basavaraja *et al* 2010; Chakraborty *et al* 2012; Duran and Bereket 2012) and its derivatives such as poly(*N*-methylpyrrole) (P(*N*-MPy)) are conducting polymers due to their electrical properties and usable as protective coatings on oxidible metals (Asan *et al* 2005). *N*-MPy has advantages compared to pyrrole due to a methyl group, which can create a hydrophobic effect (Rajagopalan *et al* 2003). Methyl groups may also decrease the adhesion strength on the electrode surface. Copolymerization is also very useful for tailoring diverse properties of coatings on the electrode surface. The obtained polymer will have different properties depending on the ratio of monomer feed ratios (Tüken *et al* 2007).

Polythiophenes are the better characterized amongst conducting polymers due to their effective solubility properties. Polymerization of the thiophene ring can result in linkage at the α- or β-position (Marino 1971; Kellogg 1979; Tanaka *et al* 1986; Taylor 1986; Laguren-Davideon *et al* 1988). The number of α,α-linkages in the polymer chains can be increased by using β-position-substituted thiophene monomers such as 3-alkylthiophenes or bithiophene (Tourillon and Garnier 1983; Wei *et al* 1991). Polybithiophene (PBTh), which is the simplest conducting polymer of the thiophene derivatives, is easily polymerized by the electrochemical technique (Zhang *et al* 2001; Vu *et al* 2005). The electropolymerization of bithiophene (BTh) often results in PBTh films with a more structurally ordered polymer (Diagne *et al* 2007) and compact structures (Elhames *et al* 2009). The potential of the polymerization of bithiophene is lower than that of thiophene. This allows one to decrease the degradation that accompanies anodic synthesis of the conducting polymer (CP) and diminishing of the irreversibility of redox conversions of such polymers (Alpatova *et al* 2004). BTh and *N*-methylpyrrole have been used as suitable candidates for copolymerization. The choice of PBTh has been suggested by the literature reports claiming that a polymer could form homogeneous films, which are stable against

*Author for correspondence (mates@nku.edu.tr)

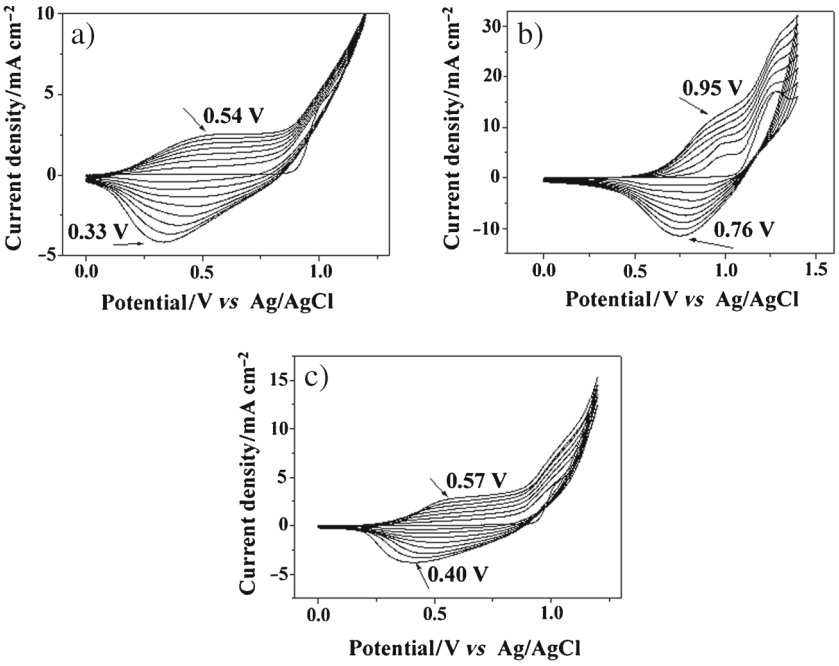

Figure 1. Cyclic voltammetry of (**a**) *N*-MPy (Q = 20·59 mC), potential range: 0–1·2 V, $[N\text{-MPy}]_0$ = 20 mM, (**b**) 2,2′ -BTh (Q = 50·05 mC), potential range: 0–1·4 V, $[\text{BTh}]_0$ = 20 mM and (**c**) P(*N*-MPy-co-BTh) (Q = 21·71 mC), potential range: 0–1·2 V, $[N\text{-MPy}]_0/[\text{BTh}]_0 = 1/5$ on a glassy carbon electrode (GCE) in 0·2 M $NaClO_4/CH_3CN$, 8 cycle, scan rate: 100 mV s^{-1}.

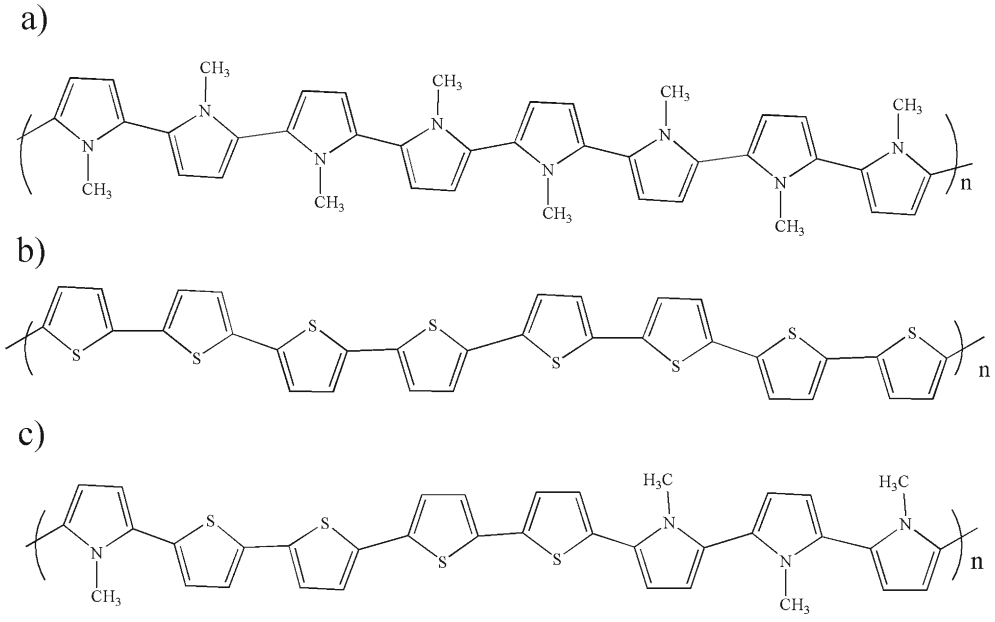

Figure 2. Polymer structures of (**a**) P(*N*-MPy), (**b**) P(BTh) and (**c**) P(*N*-MPy-co-BTh) on a glassy carbon electrode in 0·2 M $NaClO_4/CH_3CN$.

atmospheric oxidation at room temperature (Morgen *et al* 1995).

Electrochemical copolymerization has recently been widely applied to the synthesis of conductive polymers. It is one strategy for developing new materials by combining the individual properties of polymers by linking two different monomers into a polymer chain (Torres and Fox 1992). Thus, the copolymer is expected to gain both

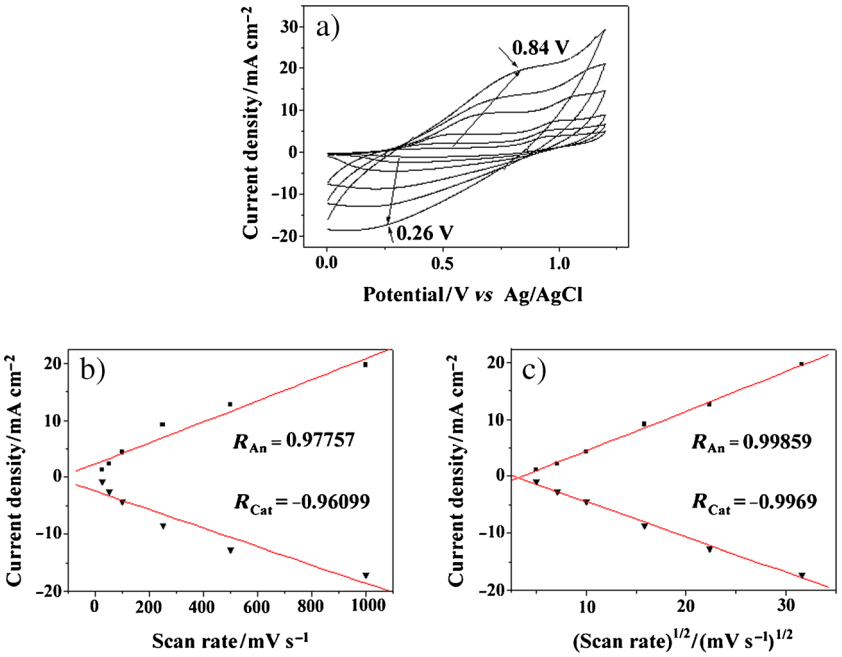

Figure 3. Cyclic voltammetry of (**a**) P(*N*-MPy-co-BTh)/GCE in a monomer-free solution in 0·2 M $NaClO_4/CH_3CN$, (**b**) scan rate vs current density and (**c**) square root of scan rate vs current density plot $[N\text{-MPy}]_0/[\text{BTh}]_0 = 1/5$, 8 cycle, scan rate: 25–1000 mV s^{-1}, potential range: 0–1·2 V.

conductivity and good mechanical properties from its two components (Zinger and Kijel 1991; Ustamehmetoglu *et al* 2003). Electrochemical impedance spectroscopy (EIS) is an effective and reliable method to extract information about electrochemical characteristics of the electrochemical system (Cebeci *et al* 2009). Double-layer capacitance, diffusion impedance, determination of the rate of charge transfer and charge transport processes and solution resistance of the electrochemical system can be achieved by EIS (Barsoukov and Macdonald 2005). EIS is also considered as one of the best techniques for analysing the properties of conducting polymer electrodes (Ates and Uludag 2011; Bisquert and Compte 2001). There are two principal approaches to modelling the impedance of such systems: a uniform, homogeneous film (Buck and Mundt 1999; Lang and Inzelt 1999) and a porous membrane (Ehrenbeck *et al* 1998; Nguyen and Passch 1999).

Dang *et al* (2004) studied electrochemical copolymerization of pyrrole and bithiophene. They reported that cyclic voltammograms showed that the electrochemical properties of the resulting copolymer films gradually changed the ratio of polypyrrole to polybithiophene, with an increase in concentration of bithiophene in the initial electrolyte. They carried out electrochemical impedance and photocurrent measurements in order to identify the semiconducting properties of the homopolymers and copolymers.

This study reports electrochemical random copolymerization of *N*-MPy and BTh in various initial feed ratios. Homo- and co-polymers were characterized by CV, FTIR–ATR, SEM–EDX and EIS analysis. The electrochemical impedance data were fitted to the equivalent circuit model of R(C(R)(QR)(CR)) in order to explain the double-layer capacitance and electrical parameters.

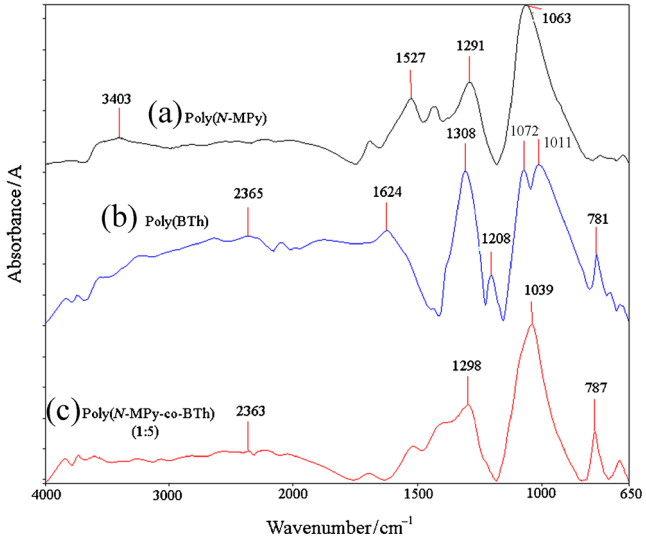

Figure 4. FTIR-ATR spectra: Admittance (*A*) vs wavenumber (cm^{-1}) for (**a**) P(*N*-MPy)/CFME, $[N\text{-MPy}]_0 = 20$ mM, potential range: 0 V^2 − +1·2 V, scan rate: 100 mV s^{-1}, 0·2 M $NaClO_4/CH_3CN$, 30 cycle, $Q = 1{\cdot}551$ mC, (**b**) P(BTh)/CFME, $[\text{BTh}]_0 = 20$ mM, potential range: 0− + 1·4 V, scan rate: 100 mV s^{-1}, 0·2 M $NaClO_4/CH_3CN$, 30 cycle, $Q = 2{\cdot}082$ mC and (**c**) P(*N*-MPy-co-BTh)/CFME, $[N\text{-MPy}]_0/[\text{BTh}]_0 = 1/5$, potential range: 0−+1·2 V, scan rate: 100 mV s^{-1}, 0·2 M $NaClO_4/CH_3CN$, 30 cycle, $Q = 2{\cdot}732$ mC.

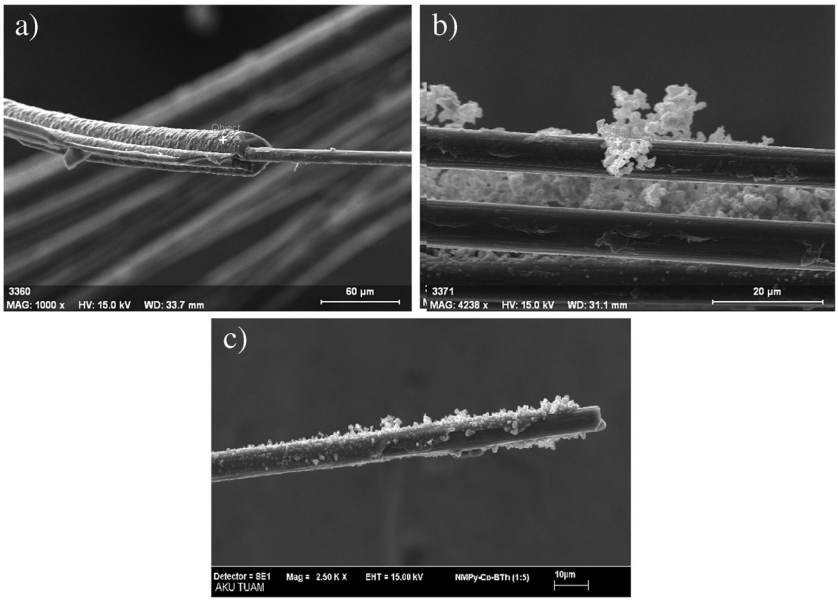

Figure 5. SEM point analysis of (**a**) P(*N*-MPy) on a single CFME, $[N\text{-MPy}]_0 = 20$ mM, potential range: $0- + 1{\cdot}2$ V, scan rate: 100 mV s^{-1}, 0·2 M $NaClO_4/CH_3CN$, 30 cycle, $Q = 655{\cdot}4$ mC, (**b**) P(BTh) on a single CFME $[BTh]_0 = 20$ mM, potential range: $0 - +1{\cdot}4$ V, scan rate: 100 mV s^{-1}, 0·1 M $NaClO_4/CH_3CN$, 30 cycle, $Q = 1{\cdot}060$ mC and (**c**) P(*N*-MPy-co-BTh) on a single CFME, $[N\text{-MPy}]_0/[BTh]_0 = 1/5$, potential range: $0 - +1{\cdot}4$ V, scan rate: 100 mV s^{-1}, 0·2 M $NaClO_4/CH_3CN$, 30 cycle, $Q = 2{\cdot}732$ mC.

2. Experimental

2.1 *Materials*

The monomers of *N*-methylpyrrole (*N*-MPy) and 2,2′-bithiophene (BTh) were provided by Sigma-Aldrich. All other reagents included acetonitrile (Aldrich, 99·93%) and the supporting electrolytes of sodium perchlorate (Aldrich >98·0%) were used without any treatment or further purification.

2.2 *Instrumentation*

Cyclic voltammetry (CV) was performed using PARSTAT 2273 (software: Powersuit and Faraday cage: BASI Cell Stand C3) in a three-electrode configuration, which employed a glassy carbon electrode (GCE) (area: 0·07 cm^2) as working electrode, platinum wire as counter electrode and Ag|AgCl|0·3 M KCl as reference electrode. The working electrode was carefully polished with alumina slurry and cleaned in an ultrasonic bath before each experiment.

A modified carbon fibre microelectrode (CFME) was characterized by Fourier transform infrared-attenuated transmittance reflectance (FTIR-ATR) spectroscopy (Perkin Elmer, Spectrum One B, with an universal ATR attachment with a diamond and ZnSe crystal). Morphological investigations were performed with scanning electron microscopy (SEM) and energy dispersive X-ray analysis (EDX) using a Carl Zeiss Leo 1430 VP.

Electrochemical impedance spectroscopic (EIS) measurements were performed in 0·2 M $NaClO_4$/acetonitrile (CH_3CN). EIS measurements were done in a monomer-free electrolyte solution with a perturbation amplitude of 10 mV r.m.s. over a frequency range of 0·01 – 100·000 Hz with PARSTAT 2273 model Potentiostat/galvanostat.

3. Results and discussion

3.1 *Electropolymerization of N-MPy and BTh on GCE*

CV of *N*-MPy showed one oxidation peak at +0·54 V and a reduction peak at +0·33 V, which have the electroactivity of a monomer (figure 1a). An increase in the peak intensities was observed upon eight cycles. CV of BTh has higher oxidation potential (+0·95V) and higher reduction peak potential (+0·76V) than P(*N*-MPy) (figure 1b). After increasing the bithiophene monomer concentration of the electrochemical cell, which includes N-MPy monomer, the electro-active copolymer formation had an oxidation peak at +0·57 V and one reduction peak at +0·40 V (figure 1c). The monomer concentration of BTh is five times higher than *N*-MPy. This redox behaviour completely differed from those of both monomers. The oxidation and reduction peak potential values exist between the peak potential values of the *N*-MPy and BTh monomers.

N-MPy and BTh monomers only formed homopolymers with their monomers (figures 2a and b). However, they need

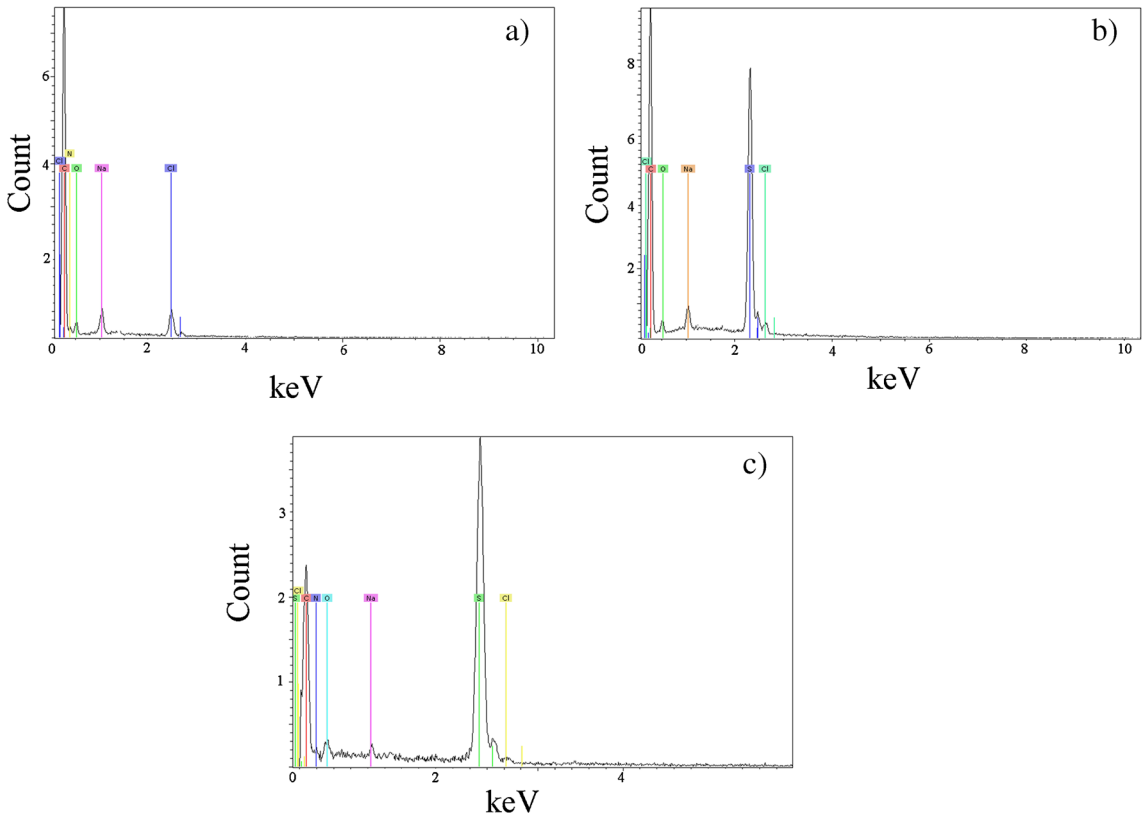

Figure 6. EDX point analysis of (**a**) P(*N*-MPy) on a single CFME, $[N\text{-MPy}]_0 = 20$ mM, potential range: 0−+ 1·2 V, scan rate: 100 mV s^{-1}, 0·2 M $NaClO_4/CH_3CN$, 30 cycle, $Q = 655{\cdot}4$ mC, (**b**) P(BTh) on a single CFME, $[BTh]_0 = 20$ mM, potential range: 0− + 1·4 V, scan rate: 100 mV s^{-1}, 0 · 1 M $NaClO_4/CH_3CN$, 30 cycle, $Q = 1 \cdot 060$ mC and (**c**) P(*N*-MPy-co-BTh) on a single CFME, $[N\text{-MPy}]_0/[BTh]_0 = 1/5$, potential range: 0− + 1·4 V, scan rate: 100 mV s^{-1}, 0·2 M $NaClO_4/CH_3CN$, 30 cycle, $Q = 1{\cdot}002$ mC.

Table 1. EDX percent amount analysis of P(*N*-MPy), P(BTh) and P(*N*-MPy-co-BTh)/CFME.

			P(*N*-MPy-co-BTh)			
Elements / K series	P(*N*-MPy)	P(BTh)	$[N\text{-MPy}]_0/[BTh]_0 = 1/1$	$[N\text{-MPy}]_0/[BTh]_0 = 1/2$	$[N\text{-MPy}]_0/[BTh]_0 = 1/5$	$[N\text{-MPy}]_0/[BTh]_0 = 1/10$
Carbon	48·33	58·91	36·11	28·19	31·42	43·00
Nitrogen	21·63	–	24·56	20·96	20·97	18·97
Oxygen	23·14	23·50	28·11	34·34	28·86	23·95
Sodium	3·384	1·79	1·35	1·82	1·04	1·68
Chlorine	3·51	0·95	–	3·23	0·23	0·40
Sulfur	–	14·86	9·87	11·45	17·48	11·04

to be mixed in a non-regular or random pattern to create a random copolymer as shown in figure 2c.

3.2 *Effect of scan rate in a monomer-free solution*

The scan rate dependence of the electro-active film was investigated on the reversible system of oxidation peak potential at ∼0·84 V and reduction peak potential at ∼0·26 V (figure 3a). The peak current density (i_p) for a reversible voltammogram at standard room temperature is given by the following equation:

$$i_p = (2{\cdot}69 \times 10^5) \times A \times D^{1/2} \times C_0 \times \nu^{1/2},$$

where ν is the scan rate, A the electrode area and D the diffusion coefficient of the electro-active species in the solution. The scan rate dependence of the anodic and cathodic peak current densities shows a linear dependence on scan rates from 25 to 1000 mV s^{-1} (R_{1an} = 0·97757 and

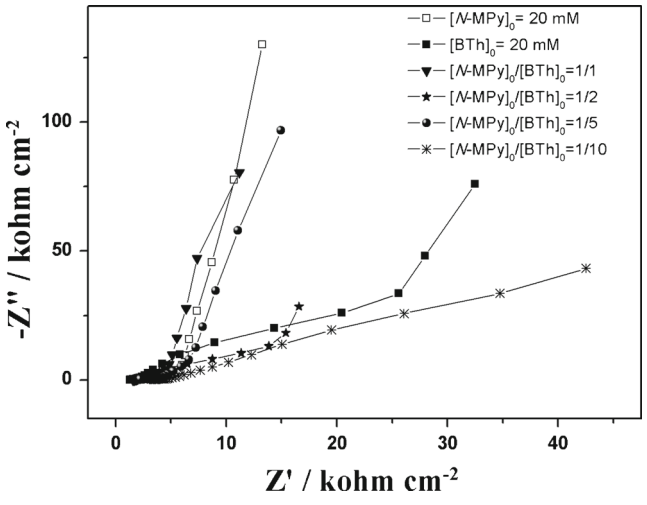

Figure 7. Nyquist plot of P(*N*-MPy)/GCE, $[N\text{-MPy}]_0 = 20$ mM; P(BTh)/GCE, $[\text{BTh}]_0 = 20$ mM, and P(*N*-MPy-co-BTh), $[N\text{-MPy}]_0/[\text{BTh}]_0 = 1/1, 1/2, 1/5$ and 1/10. Electrodeposition was done on GCE in 0·2 M $NaClO_4/CH_3CN$ at a scan rate of 100 mV s^{-1} using multiple cycles (8 cycles) and potential range: 0–1·4 V.

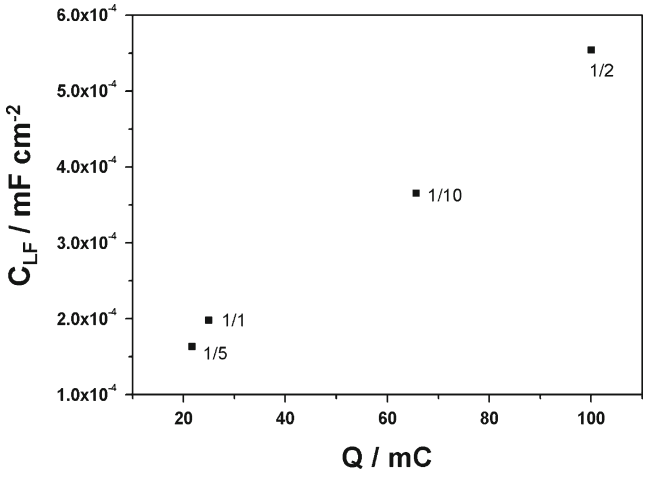

Figure 8. Correlation between low-frequency capacitance (C_{LF}/mF cm^{-2}) and total charges (Q/mC) obtained during electrogrowth process.

$R_{1cat} = -0{\cdot}96099$) for poly(*N*-MPy-co-BTh)/GCE, $[N\text{-MPy}]_0/[\text{BTh}]_0 = 1/5$ (figure 3b). The peak current density was determined to be proportional with $\nu^{1/2}$ in the range of the square root of scan rates from 5 to 22·36 mV s^{-1} (regression fit (R_{2an}) = 0·99859 and $R_{2cat} = -0{\cdot}9969$), where diffusion control applies (Vorotyntsev *et al* 1994) (figure 3c). This demonstrates that the electrochemical process has diffusion controlled process.

3.3 *FTIR–ATR measurements*

FTIR–ATR spectra of P(*N*-MPy), P(BTh) and P(*N*-MPy-co-BTh) were obtained from the surface of the electro-coated CFMEs by reflectance measurements. The absorption bands

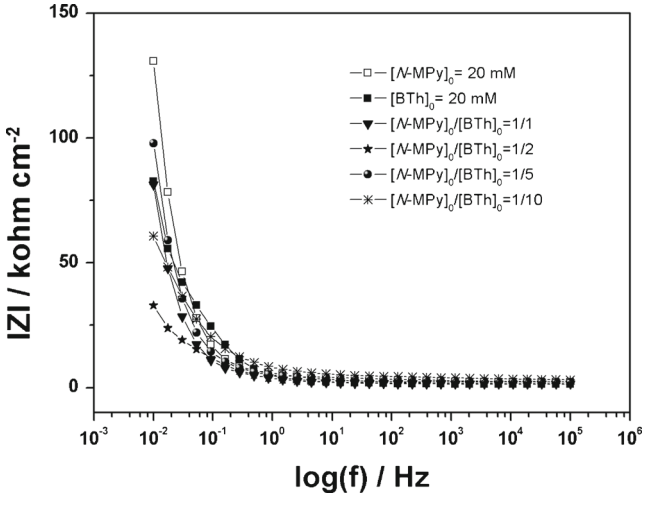

Figure 9. Bode magnitude plot of P(*N*-MPy)/GCE, $[N\text{-MPy}]_0 = 20$ mM; P(BTh)/GCE, $[\text{BTh}]_0 = 20$ mM; P(*N*-MPy-co-BTh), $[N\text{-MPy}]_0/[\text{BTh}]_0 = 1/1, 1/2, 1/5$ and 1/10. Electrodeposition was done on GCE in 0·2 M $NaClO_4/CH_3CN$ at a scan rate of 100 mV s^{-1} using multiple cycles (8 cycles) and potential range: 0–1·4 V.

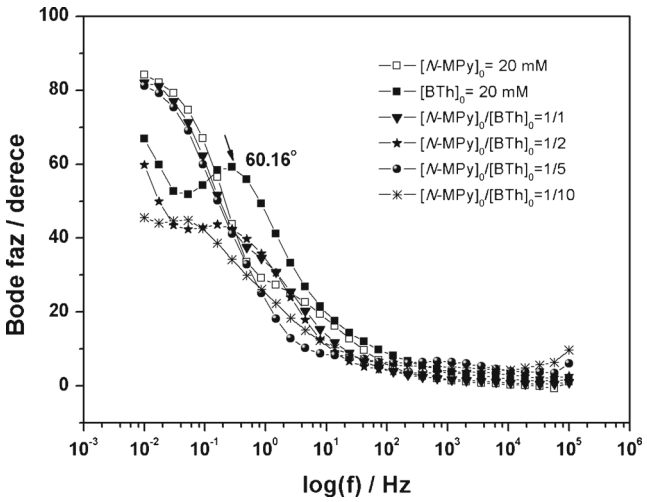

Figure 10. Bode phase plot of P(*N*-MPy)/GCE, $[N\text{-MPy}]_0 = 20$ mM; P(BTh)/GCE, $[\text{BTh}]_0 = 20$ mM; P(*N*-MPy-co-BTh), $[N\text{-MPy}]_0/[\text{BTh}]_0 = 1/1, 1/2, 1/5$ and 1/10. Electrodeposition was done on GCE in 0·2 M $NaClO_4/CH_3CN$ at a scan rate of 100 mV s^{-1} using multiple cycles (8 cycles) and potential range: 0–1·4 V.

of each spectrum are given in figure 4. P(*N*-MPy) has the following characteristic peaks: 1537 cm^{-1}, (aromatic C=C), 1291 cm^{-1} (C–N), 1063 cm^{-1} (ClO_4^- from the electrolyte of $NaClO_4$). The peak at 3403 cm^{-1} belongs to $-CH_3$ (sp^3, C–H stretching) (Sarac *et al* 2006a). The characteristic peak of C–N from *N*-MPy is given at 1291 cm^{-1} (the valence vibration of the C–N bond of *N*-MPy) (Sarac *et al* 2006b). In the literature, FTIR spectrum of the copolymer of 1,4-bis(2-thienyl)-naphtlane with 2,2′-bithiophene was given, which shows similar peaks in the FTIR–ATR spectrum for P(BTh) (Cui *et al* 2011). Some shifts or new peak formations co-

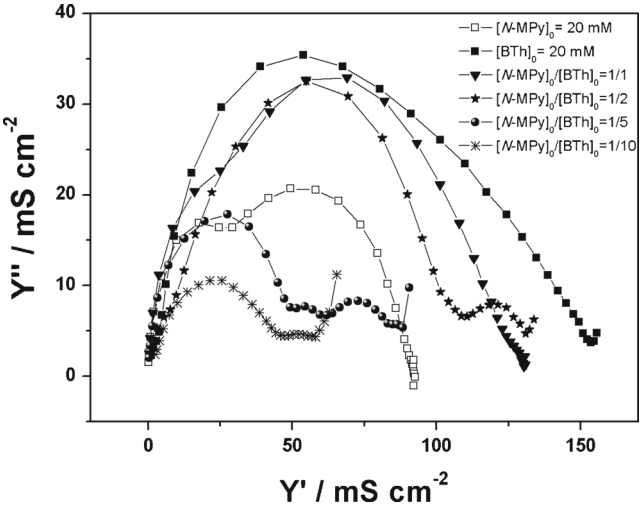

Figure 11. Admitance plot of P(*N*-MPy)/GCE, $[N\text{-MPy}]_0 = 20$ mM; P(BTh)/GCE, $[\text{BTh}]_0 = 20$ mM; P(*N*-MPy-co-BTh), $[N\text{-MPy}]_0/[\text{BTh}]_0 = 1/1, 1/2, 1/5$ and 1/10. Electrodeposition was done on GCE in 0·2 M $NaClO_4/CH_3CN$ at a scan rate of 100 mV s^{-1} using multiple cycles (8 cycles) and potential range: 0–1·4 V.

rrespond to combination of the monomers. P(BTh) has the following characteristic peaks: 1624 cm^{-1} (aromatic C=C), 1308 cm^{-1} (aromatic C–C), 1203 cm^{-1} (aromatic C–H) and 1011 cm^{-1} (ClO_4^- from the electrolyte of $NaClO_4$), 781 cm^{-1} (C–S). The characteristic peak at 781 cm^{-1} refers to the C–S bond for P(BTh). However, this peak does not exist in P(*N*-MPy).

These peaks are included in the copolymer structure by the following peak, 787 cm^{-1}, in the initial feed ratio of $[N\text{-MPy}]_0/[\text{BTh}]_0 = 1/5$. In the literature, C–S stretching appeared at 793 and 632 cm^{-1} (Kham *et al* 2004; Beyazyildirim *et al* 2006). The characteristic peaks at 1291 cm^{-1} (C–N) comes from P(*N*-MPy) and 781 cm^{-1} (C–S) comes from P(BTh). These two important peaks are incorporated into the copolymer structure. This is the strong evidence of copolymer formation. In addition, the peak at 1039 cm^{-1} refers to the dopant ion of ClO_4^-.

3.4 *SEM measurements*

The surface morphology of the electrochemically formed *N*-methylpyrrole, 2,2′-bithiophene and copolymer of BTh and *N*-MPy/carbon fibre microelectrodes interphases varied in the initial feed ratio of $[N\text{-MPy}]_0/[\text{BTh}]_0 = 1/1, 1/2, 1/5$ and 1/10 used as shown in figure 5(a–f). The coatings with micro-spherical morphology were formed using the solution of 0·2 M $NaClO_4/CH_3CN$. In previous studies, Diaz *et al* (1984) reported that the physical structure differences of the surfaces of thin films formed by electrochemical polymerization did not affect surface energies of the films. Iroh and Wood (1996) reported a correlation between surface energy and morphology of carbon fibres coated with polypyrrole by aqueous electrochemical polymerization. Many process parameters, such as the polymer concentration, electrolyte concentration, type of electrolyte, applied voltage and polymerization time affect surface energy of the coated fibres. The total charges were obtained during the electro-growth process as 20·59 mC for P(*N*-MPy), 50·05 mC for PBTh and 25·02, 100·1, 21·71, 65·66 mC for P(*N*-MPy-co-BTh) in a feed ratio of $[N\text{-MPy}]_0/[\text{BTh}]_0 = 1/1, 1/2, 1/5$ and 1/10, respectively. The highest charge (100·1 mC) was obtained for a copolymer in the feed ratio of $[N\text{-MPy}]_0/[\text{BTh}]_0 = 1/2$. SEM image shows more coatings on the carbon fibre surface. In addition, the low-frequency capacitance of the copolymer was obtained for the highest value of $C_{LF} = 5{\cdot}54 \times 10^{-4}$ mF cm^{-2} in the initial feed ratio of $[N\text{-MPy}]_0/[\text{BTh}]_0 = 1/2$.

3.5 *EDX analysis*

Energy dispersive X-ray analysis (EDX) provides important evidence of polymer film formation, as shown in figure 6(a–c). There is no sulfur element in the structure of P(*N*-MPy). The nitrogen element is not included in the P(BTh). However, these two elements exist in the copolymer structure in different percentages, as shown in table 1. The highest percentage of sulfur and nitrogen elements exists in the initial feed ratio of $[N\text{-MPy}]_0/[\text{BTh}]_0 = 1/5$. Sodium and chlorine elements prove that the dopant ion is included in the polymer structure from the electrolyte of $NaClO_4$.

3.6 *Electrochemical impedance spectroscopy*

Electrochemical impedance spectroscopy (EIS) is an important technique used to obtain electrochemical information and capacitive behaviour of a polymer/electrolyte system, such as electrolyte resistance, charge transfer resistance and Faradaic capacitance (Popkinov *et al* 1997; Ates and Sarac 2009). The low-frequency capacitance (C_{LF}) values can be obtained from a Nyquist plot with the equation

$$C_{LF} = 1/2\pi f z''.$$

The results are as follows: $C_{LF} = 1{\cdot}23 \times 10^{-4}$ mF cm^{-2} for P(*N*-MPy), $C_{LF} = 2{\cdot}09 \times 10^{-4}$ mF cm^{-2} for P(BTh), $C_{LF} = 1{\cdot}98 \times 10^{-4}$ mF cm^{-2} for P(*N*-MPy-co-BTh) in the feed ratio of $[N\text{-MPy}]_0/[\text{BTh}]_0 = 1/1$, $C_{LF} = 5{\cdot}54 \times 10^{-4}$ mF cm^{-2} for $[N\text{-MPy}]_0/[\text{BTh}]_0 = 1/2$, $C_{LF} = 1{\cdot}63 \times 10^{-4}$ mF cm^{-2} for $[N\text{-MPy}]_0/[\text{BTh}]_0 = 1/5$, $C_{LF} = 3{\cdot}65 \times 10^{-4}$ mF cm^{-2} for $[N\text{-MPy}]_0/[\text{BTh}]_0 = 1/10$ (figure 7). The highest C_{LF} was obtained as $5{\cdot}54 \times 10^{-4}$ mF cm^{-2} for the copolymer in the feed ratio of $[N\text{-MPy}]_0/[\text{BTh}]_0 = 1/2$. It may result in a more convenient combination to form random copolymer formation in the initial feed ratio of $[N\text{-MPy}]_0/[\text{BTh}]_0$.

This result may be related to the total charges obtained during electrogrowth process. The highest total charge ($Q = 100{\cdot}1$ mC) was obtained for the copolymer in the initial feed ratio of $[N\text{-MPy}]_0/[\text{BTh}]_0 = 1/2$ compared to other feed ratios of $[N\text{-MPy}]_0/[\text{BTh}]_0 = 1/1$ ($Q = 25{\cdot}02$ mC), $[N\text{-MPy}]_0/[\text{BTh}]_0 = 1/5$ ($Q = 21{\cdot}71$ mC) and $[N\text{-MPy}]_0/[\text{BTh}]_0 = 1/10$ ($Q = 65{\cdot}66$ mC). Figure 8 shows C_{LF} and Q graph.

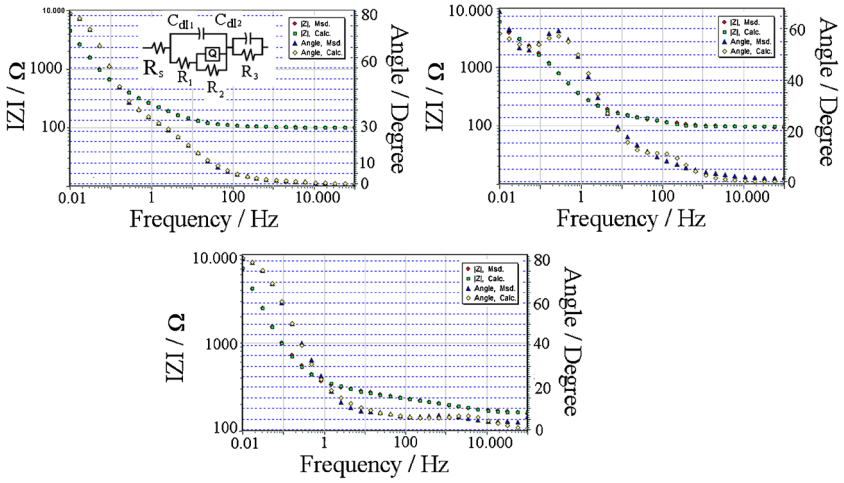

Figure 12. Bode-magnitude and phase plot for (**a**) poly(*N*-MPy), $[N\text{-MPy}]_0$ = 20 mM, (**b**) poly(BTh), $[\text{BTh}]_0$ = 20 mM and (**c**) poly(*N*-MPy-co-BTh), $[N\text{-MPy}]_0/[\text{BTh}]_0$ = 1/5 electro-coated on CFME. Inset of **a**. Equivalent circuit model of R(C(R)(QR)(CR).

Table 2. Circuit model of R(C(R(QR)))(CR) were analyzed electrochemically P(*N*-MPy), P(BTh), and P(*N*-MPy-co-BTh)/GCE in the initial feed ratio of $[N\text{-MPy}]_0/[\text{BTh}]_0$ = 1/1, 1/2, 1/5 and 1/10 with ZSimpWin simulating programme. Monomers were electro-coated on GCE at a scan rate of 100 mV s^{-1}, using multiple (8 cycle) in 0·2 M $NaClO_4/CH_3CN$.

Components R(C(R(QR)))(CR)	P(*N*-MPy)	P(BTh) $[\text{BTh}]_0$	$[N\text{-MPy}]_0/[\text{BTh}]_0 = 1/1$	$[N\text{-MPy}]_0/[\text{BTh}]_0 = 1/2$	$[N\text{-MPy}]_0/[\text{BTh}]_0 = 1/5$	$[N\text{-MPy}]_0/$ = 1/10
$R_s/(\Omega)$	99·27	96·57	110·2	109·6	162·3	185·2
$C_1/(\mu F)$	15·10	33·60	18·60	3·13	0·91	2·92
$R_1/(\Omega)$	3·94	39·58	8·77	21·13	19·09	57·75
Q/mV s^{-1}	1·58	1·25	1·50	2·48	3·50	1·10
n	0·62	0·71	0·68	0·62	0·26	0·56
$R_2/(\Omega)$	364·1	6·41	304·1	669·1	657·4	151·0
C_2/(mF)	3·57	2·53	2·80	4·00	2·30	3·31
$R_3/(\Omega)$	$7{\cdot}32 \times 10^4$	586·2	$8{\cdot}92 \times 10^4$	185·3	$1{\cdot}20 \times 10^5$	62·88
χ^2	$7{\cdot}18 \times 10^{-5}$	$3{\cdot}87 \times 10^{-3}$	$2{\cdot}2 \times 10^{-4}$	$2{\cdot}61 \times 10^{-3}$	$1{\cdot}63 \times 10^{-3}$	$9{\cdot}75 \times 10^{-4}$

Double-layer capacitance (C_{dl}) can be calculated from the Bode-magnitude plot of the equation IZI = $1/C_{dl}$ by extrapolating the linear section to the value of $\omega = 1$ ($\log \omega = 0$) (Inzelt 2003). Double-layer capacitance of the system was obtained as $C_{dl} = \sim 0{\cdot}20\ \mu F\,cm^{-2}$ for P(*N*-MPy), ($C_{dl} = \sim 0{\cdot}17\ \mu F\,cm^{-2}$) for P(BTh) and $C_{dl} = \sim 0{\cdot}29$, 0·27, 0·22 and 0·12 μF cm^{-2} for the copolymer in the initial feed ratios of $[N\text{-MPy}]_0/[\text{BTh}]_0$ = 1/1, 1/2, 1/5 and 1/10, respectively (figure 9). C_{dl} values of the copolymer, especially in the initial feed ratio of $[N\text{-MPy}]_0/[\text{BTh}]_0$ = 1/1, 1/2 and 1/5 are higher than the homopolymers.

The phase angles were determined from the Bode-phase plot as shown in figure 10. The phase angle was obtained at 60·16° at the frequency of 0·28 Hz for P(BTh). The highest phase angles ($\theta = 83{\cdot}88°$) were obtained at the frequency of 0·011 Hz for P(*N*-MPy). The phase angle ($\theta = 67{\cdot}32°$) was obtained for P(BTh) at the frequency of 0·01 Hz. The phase angle ($\theta = 81{\cdot}96°$) was obtained for P(*N*-MPy-co-BTh) in the initial feed ratio of $[N\text{-MPy}]_0/[\text{BTh}]_0$ = 1/1 at the frequency of 0·010 Hz. However, if the frequency decreases, the phase angle increases to 60·16° at the frequency of 0·28 Hz for P(BTh). The minimum phase angles were ($\theta = 8{\cdot}83°$ at 41·9 Hz for P(*N*-MPy), $\theta = 11{\cdot}5°$ at 41·9 Hz for P(BTh), and $\theta = 4{\cdot}94°$ at 44·14 Hz for P(*N*-MPy-co-BTh) in the initial feed ratio of $[N\text{-MPy}]_0/[\text{BTh}]_0$ = 1/2. At higher frequencies, the highest phase angle ($\theta = 9{\cdot}20°$) was obtained at the frequency of 94658·7 Hz for the copolymer in the initial feed ratio of $[N\text{-MPy}]_0/[\text{BTh}]_0$ = 1/2.

The lowest conductivity results were obtained for P(*N*-MPy-co-BTh)/GCE in the feed ratio of $[N\text{-MPy}]_0/[\text{BTh}]_0$ = 1/10 according to the admittance plot as shown in figure 11. The admittance plot is correlated with the Bode-magnitude

plot. The conductivity of the polymer films is in the order of P(BTh) > P(*N*-MPy-co-BTh) for $[N\text{-MPy}]_0/[\text{BTh}]_0 = 1/1 > [N\text{-MPy}]_0/[\text{BTh}]_0 = 1/2 >$ P(*N*-MPy) > $[N\text{-MPy}]_0/[\text{BTh}]_0 = 1/5 > [N\text{-MPy}]_0/[\text{BTh}]_0 = 1/10$.

3.7 *Equivalent circuit model evaluation*

The equivalent electrical circuit model of R(C(R(QR)))(CR) was given for the electrolyte/poly(*N*-MPy-co-BTh)/GCE system to a frequency range of 0·01–100·000 Hz. The ZSimpWin 3·10 circuit model programme from Princeton Applied Research was evaluated to fit the theoretical and experimental circuits. Kramers–Kronig (K–K) transforms were performed in the analysis of impedance data with reference to the conditions of stability and linearity (Urquidi-Macdonald *et al* 1990). Using the K–K transforms, the real part of a transfer function can be calculated for a casual, stable, linear time invariant and a finite system when $f \to 0$ and $f \to \infty$, when the change in its imaginary part, as a function of frequency, is known. Alternatively, the imaginary part of a transfer function can be calculated when the evolution of its real part is known (Diard *et al* 1994). As the measurement model is consistent with the K–K relations, it enables the user to check consistency of the experimental data without using the K–K relations (Shukla *et al* 2004).

This study used the circuit model of R(C(R(QR)))(CR) for P(*N*-MPy), P(BTh) and P(*N*-MPy-co-BTh) as shown in figure 12(a–c), respectively. The circuit model was previously used in the author's poly(9-benzyl-9*H*-carbazole) paper (Ates and Uludag 2011). R_s is the solution resistance of the modified electrode and electrolyte of $NaClO_4$. C_1 is the double-layer capacitance and R_1 is the charge transfer resistance between the polymer film and the electrolyte interface. The series connection to R_1 consists of the constant phase element (Q) in parallel with R_2 (resistance of polymer film). The second components, R_3 and C_{dl2} belong to the capacitor element and the charge transfer resistance from the electrode of glassy carbon (Ates 2011b). The circuit components are shown in table 2. The solution resistance as $R_s = 99{\cdot}27\ \Omega$ for P(*N*-MPy) and $R_s = 96{\cdot}57\ \Omega$ for P(BTh) have nearly the same value. If one compares results of the R_s values of the homopolymers with copolymer, the former have lower values ($R_s = 110{\cdot}2$, 109·6, 162·3 and 185·2) for P(*N*-MPy-co-BTh) in the feed ratio of $[N\text{-MPy}]_0/[\text{BTh}]_0 = 1/1, 1/2, 1/5$ and 1/10, respectively than the copolymers. The double-layer capacitance values of the homopolymers are higher than the copolymer due to its non-ideal electrode behaviour. It should be checked from the constant phase element value (Q). For ideal electrodes, Q is equal to C_{dl} and $n = 1$. However, in this polymer/electrolyte system, especially for the copolymer, Q is $< 0{\cdot}5$ ($n = 0{\cdot}26$ for the copolymer). Usually the n value changes between 0·5 and 1, which changes the variation of the surface roughness and the heterogeneity of the surface (Vorotyntsev *et al* 1999). The C_2 values have nearly the same values. However, the R_3 value for the copolymer in the initial feed ratio of $[N\text{-MPy}]_0/[\text{BTh}]_0 = 1/1$ and 1/5 is higher than its homopolymers and copolymer in the initial feed ratio of $[N\text{-MPy}]_0/[\text{BTh}]_0 = 1/2$ and 1/10.

4. Conclusions

In this paper, the copolymers of *N*-methylpyrrole (*N*-MPy) and 2,2′-bithiophene (BTh) were electropolymerized on a glassy carbon electrode with various initial feed ratios ($[N\text{-MPy}]_0/[\text{BTh}]_0 = 1/1, 1/2, 1/5$ and 1/10. The modified films were characterised by CV, FTIR–ATR, SEM–EDX, and EIS analyses. The equivalent circuit model of R(C(R(QR)))(CR) was applied together with Kramers–Kronig transformation tests to EIS data of the polymer/electrolyte system. Finally, the equivalent circuit model is validated by a comparison between simulated results and experimental data, which shows a good fit. As a result, the highest low-frequency capacitance $C_{LF} = 5{\cdot}54 \times 10^{-4}$ mF cm^{-2} was obtained for P(*N*-MPy-co-BTh) in the initial feed ratio of $[N\text{-MPy}]_0/[\text{BTh}]_0 = 1/2$. The capacitance values changed with changing copolymer composition.

Acknowledgments

Financial support for this work by the Research Foundation of Namik Kemal University, Turkey, (project number: NKUBAP.00.10.YL.12.02), is gratefully acknowledged.

References

Akoudad S and Roncali J 1999 *J. Synth. Met.* **101** 149

Alvi F, Basnayaka P A, Ram M K, Gomez H, Stefanako E, Goswami Y and Kumar A 2012 *J. New Mater. Electrochemi. Syst.* **15** 89

Alpatova N M, Ovsyannikova E V, Topolev V V and Grosheva M Y 2004 *Russ. J. Electrochem.* **40** 229

Asan A, Kabasakaloglu M and Aksu M L 2005 *Russ. J. Electrochem.* **41** 175

Ates M and Sarac A S 2009 *Prog. Org. Coat.* **65** 281

Ates M and Uludag N 2011a *Fibers and Polymers* **12** 296

Ates M 2011b *Prog. Org. Coat.* **71** 1

Basavaraja C, Jo E A, Kim B S, Kim D G and Huh D S 2010 *Macromol. Res.* **18** 1037

Barsoukov E and Macdonald J R 2005 Impedance spectroscopy: theory, experiment and applications, (ed.) N J Hoboken (Wiley: Interscience) 2nd edn, pp. 68–73

Beyazyildirim S, Camurlu P, Yilmaz D, Gullu M and Toppare L 2006 *J. Electroanal. Chem.* **587** 235

Bisquert J and Compte A 2001 *J. Electroanal. Chem.* **499** 112

Buck R P and Mundt C 1999 *Electrochim. Acta* **44** 1999

Cebeci F Ç, Sezer E and Sarac A S 2009 *Electrochim. Acta* **54** 6354

Chakraborty G, Gupta K, Rana D and Meikap AK 2012 *Polymer Composite* **33** 343

Cui C, Xu C, Xu I, Zhao J, Liu R, Liu J, He Q and Wang H 2011 *Optical Materials* **33** 1792

Dalmolin C, Canobre S C, Biaggio S R, Rocha-Filho R C and Bocchi N 2005 *J. Electroanal. Chem.* **578** 9

Dang X D, Intelmann C M, Rammelt U and Plieth W 2004 *J. Solid State Electrochem.* **8** 727

De Bruyne A, Delplancke J L and Winand R 1997 *J. Appl. Electrochem.* **27** 867

Diagne A A, Fall M, Gue'ne M, Dieng M M, Deflorian F, Rossi S, Bonora P and Volpe CD 2007 *Compes-Rendus Chimie* **10** 558

Diard J P, Landaud P, Le Canut J M, Gorrec B L and Montella C 1994 *Electrochim. Acta* **39** 2585

Diaz A F, Hernandez R, Waltman R and Bargon J 1984 *J. Phys. Chem.* **88** 3333

Duran B and Bereket G 2012 *Ind. Eng. Chem. Res.* **51** 5246

Ehrenbeck C, Juttner K, Ludwig S and Paasch G 1998 *Electrochim. Acta* **443** 49

Elhames F H, Nessark B, Boumaza N, Bahloul A, Bouhafs D and Cheriet A 2009 *Synth. Met.* **159** 1349

Iroh J O and Wood G A 1996 *J. Appl. Polym. Sci.* **62** 761

Inzelt G 2003 *J. Solid State Electrochem.* **7** 503

Kellogg R M 1979 In Comprehensive heterocyclic chemistry, (eds.), A R Katritzkfy and C W Rees (Oxford: Pergamon Press) vol 4, p. 713

Kham K, Sadki S and Chevrot C 2004 *Synth. Met.* **145** 135

Laguren-Davideon L, Pham C V, Mark H B and Ondrus D J 1988 *J. Electrochem. Soc.* **135** 1406

Lang G and Inzelt G 1999 *Electrochim. Acta* **44** 2037

Mahmoudian M R, Alias Y, Basirum W J and Ebadi M 2011 *Curr. Appl. Phys.* **11** 368

Marino G 1971 *Adv Heterocycl. Chem.* **13** 235

McCullough R D 1998 *Adv. Mater.* **10** 93

Mollahosseini A and Noroozian E 2009 *Synth Met.* **159** 1247

Morgen T, Thies A and Schultze T W 1995 *Sens. Actuators* **A51** 103

Nguyen P H and Passch G 1999 *J. Electroanal. Chem.* **460** 63

Pokhnel B, Kamrupi I R, Adhikari B, Boruah R, Boruah M and Dolui SK 2012 *Mater. Manufac. Processes* **27** 43

Popkinov G S, Barsoukov E and Schindler R N 1997 *J. Electroanal. Chem.* **425** 209

Rajagopalan B, Wei M, Musie G T, Subramaniam B and Busch D H 2003 *Ind. Eng. Chem. Res.* **42** 6505

Sarac A S, Dogru E, Ates M and Parlak E A 2006a *Turk. J. Chem.* **30** 401

Sarac A S, Ates M and Parlak E A 2006b *J. Appl. Electrochem.* **36** 889

Saraswathi R, Hillmann A R and Martin S J 1999 *J. Electroanal. Chem.* **460** 267

Shukla P K, Orazen M E and Crisalle O D 2004 *Electrochim. Acta* **49** 2881

Skotheim T A, Reynolds J R and Elsenbaumer R L (eds.) 1998. Handbook of conducting polymers (New York: Marcel Dekker) 2nd edn

Tanaka K, Shichiri T and Yamabe T 1986 *Synth. Met.* **14** 271

Taylor R 1986. In The chemistry of heterocyclic compounds, (ed.) S Gronowitz (New York: John Wiley and Sons) **Vol 44**, Part 2, pp 1–118

Tourillon G and Garnier F 1983 *J. Phys. Chem.* **87** 2289

Torres W and Fox M A 1992 *Chem. Mater.* **4** 146

Tuan C V, Tuan M A, Hieu N V and Trung T 2012 *Curr. Appl. Phys.* **12** 1011

Tüken T, Tansuğ G, Yazici B and Erbil M 2007 *Surf. Coat. Technol.* **202** 146

Urquidi-Macdonald M, Real M S and Macdonald D D 1990 *Electrochim. Acta* **35** 1559

Ustamehmetoglu B, Kelleboz E and Sarac A S 2003 *Int. J. Polymer Anal. Charact.* **8** 255

Vorotyntsev M A, Badiali J P and Inzelt G 1999 *J. Electroanal. Chem.* **472** 7

Vorotyntsev M A, Daikhin L I and Levi M D 1994 *J. Electroanal. Chem.* **364** 37

Volpi E, Trueba M and Trasatti S P 2012 *Prog. Organi. Coat.* **74** 376

Vu Q T, Pavlik M, Hebestreit N, Pfleger J, Rammelt U and Plieth W 2005 *Electrochim. Acta* **51** 1117

Wei Y, Chan C C, Tian J, Jang G W and Hsueh K F 1991 *Chem. Mater.* **3** 888

Zhang W F, Schmidt- Zhang P and Kossmehl G 2000 *J. Solid State Electrochem.* **4** 225

Zhang W, Schmidt-Zhang P, Kossmehl G and Plieth W 1999 *J. Solid State Electrochem.* **3** 135

Zhang F, Petr A, Kirbach U and Dunsch L 2001 *Highlights* 33

Zhoor A, Qiu T, Zhang J R and Li X Y 2009 *J. Mater. Sci.* **44** 6054

Zinger B and Kijel D 1991 *Synth. Met.* **41** 1013